Comparison of the equilibrium, kinetic and water exchange properties of some metal ion-DOTA and DOTA-bis(amide) complexes

Gyula Tircsó, Enikő Tircsóné Benyó, Zoltán Garda, Jaspal Singh, Robert Trokowski, Ernő Brücher, A. Dean Sherry, Éva Tóth, Zoltán Kovács

Journal of Inorganic Biochemistry 206 (2020) 111042

Contents lists available at ScienceDirect

Journal of Inorganic Biochemistry

journal homepage: www.elsevier.com/locate/jinorgbio

Comparison of the equilibrium, kinetic and water exchange properties of some metal ion-DOTA and DOTA-bis(amide) complexes

Gyula Tircsó[a,*], Enikő Tircsóné Benyó[a], Zoltán Garda[a], Jaspal Singh[b], Robert Trokowski[b,c], Ernő Brücher[a], A. Dean Sherry[b,c], Éva Tóth[d], Zoltán Kovács[b,*]

[a] University of Debrecen, Department of Physical Chemistry, Egyetem tér 1, Debrecen H-4032, Hungary
[b] Advanced Imaging Research Center, University of Texas Southwestern Medical Center, 5323 Harry Hines Boulevard, Dallas, TX 75390, United States of America
[c] Department of Chemistry, University of Texas at Dallas, P.O. Box 830660, Richardson, TX 75083, United States of America
[d] Centre de Biophysique Moléculaire, CNRS, rue Charles Sadron, 45071 Orléans, Cedex 2, France

ARTICLE INFO

Keywords:
Coordination chemistry
Complexes
Physico-chemical parameters
Synthesis
Stability
Inertness
Water exchange rate

ABSTRACT

The 1,7-diacetate-4,10-diacetamide substituted 1,4,7,10-tetraazacyclododecane structural unit is common to several responsive Magnetic Resonance Imaging (MRI) contrast agents (CAs). While some of these complexes (agents capable of sensing fluctuations in Zn^{2+}, Ca^{2+} etc. ions) have already been tested in vivo, the detailed physico-chemical characterization of such ligands have not been fully studied. To fill this gap, we synthesized a representative member of this ligand family possessing two acetate and two n-butylacetamide pendant side-arms (DO2A2M^{nBu} = 1,4,7,10-tetraazacyclodoecane-1,7-di(acetic acid)-4,10-di(*N*-butylacetamide)), and studied its complexation properties with some essential metal and a few lanthanide(III) (Ln(III)) ions. Our studies revealed that the ligand basicity, the stability of metal ion complexes, the trend of stability constants along the Ln(III) series, the formation rates of the Ln(III) complexes and the exchange rate of the bound water molecule in the Gd(III) complex fell between those of Ln(DOTA)$^-$ and Ln(DOTA-tetra(amide))$^{3+}$ complexes (DOTA = 1,4,7,10-tetraazacyclododecane-1,4,7,10-tetraacetic acid, DOTAM = 1,4,7,10-tetrakis(carbamoylmethyl)-1,4,7,10-tetraazacyclododecane). The only exception is the stability of Cu(DO2A2M^{nBu}) which was found to be only slightly lower than that of Cu(DOTA)$^{2-}$ (log K_{CuL} = 19.85 vs. 21.98). This is likely reflects exclusive coordination of the negatively charged acetate donor atoms to the Cu^{2+} ion forming an octahedral complex with the amides remaining uncoordinated. The only anomaly observed during the study was the rates of acid assisted dissociation of the Ln(III) complexes, which occur at a rate similar to those observed for the Ln(DOTA)$^-$ complexes. These data indicate that even though the Ln(DO2A2M^{nBu})$^+$ complexes have lower thermodynamic stabilities, their kinetic inertness should be sufficient for in vivo use.

1. Introduction

Over the past three decades, various chelated forms of the lanthanide ions have found applications in different fields of biomedicine. Due to the special magnetic, optical and nuclear properties of the lanthanide (III) ions (Ln(III) ions), their complexes are widely studied as Magnetic Resonance Imaging (MRI) contrast agents (CAs) (Gd(III)), optical probes (Eu(III), Tb(III), Yb(III)) as well as diagnostic and therapeutic radiopharmaceuticals (^{90}Y, ^{153}Sm, ^{166}Ho, ^{177}Lu) [1]. The most widely used chelate in these applications has been either DOTA (1,4,7,10-tetraazacyclododecane-1,4,7,10-tetraacetic acid) or a derivative of DOTA (Fig. 1). The chemical properties of the Ln(DOTA)$^-$ complexes are in general quite favorable for biological applications because they are thermodynamically stable and kinetically inert toward dissociation [2,3]. Hence, the toxicity of these many chelated forms of the Ln(III) ions is much lower than that of the free Ln(III) ions [4–6]. Three different macrocyclic chelates of Gd(III) (Gd(DOTA)$^-$ (Dotarem), Gd(HP-DO3A) (Prohance), and Gd(DO3A-butrol) (Gadovist)) are widely used as MRI CAs (HP-DO3A = 2,2′,2″-[10-(2-hydroxypropyl)-1,4,7,10-tetraazacyclododecane-1,4,7-triyl]triacetic acid and DO3A-butrol = 10-(2,3-dihydroxy-1-hydroxymethylpropyl)-1,4,7,10-tetraazacyclododecane-1,4,7-triacetic acid). These CAs are administrated intravenously and after rapid distribution through all extracellular space are eliminated by glomerular filtration through the kidneys [7–9].

In order to modify the complexation properties of DOTA or to attach

* Corresponding authors.
E-mail addresses: gyula.tircso@science.unideb.hu (G. Tircsó), zoltan.kovacs@utsouthwestern.edu (Z. Kovács).

https://doi.org/10.1016/j.jinorgbio.2020.111042
Received 20 October 2019; Received in revised form 17 February 2020; Accepted 17 February 2020
Available online 20 February 2020

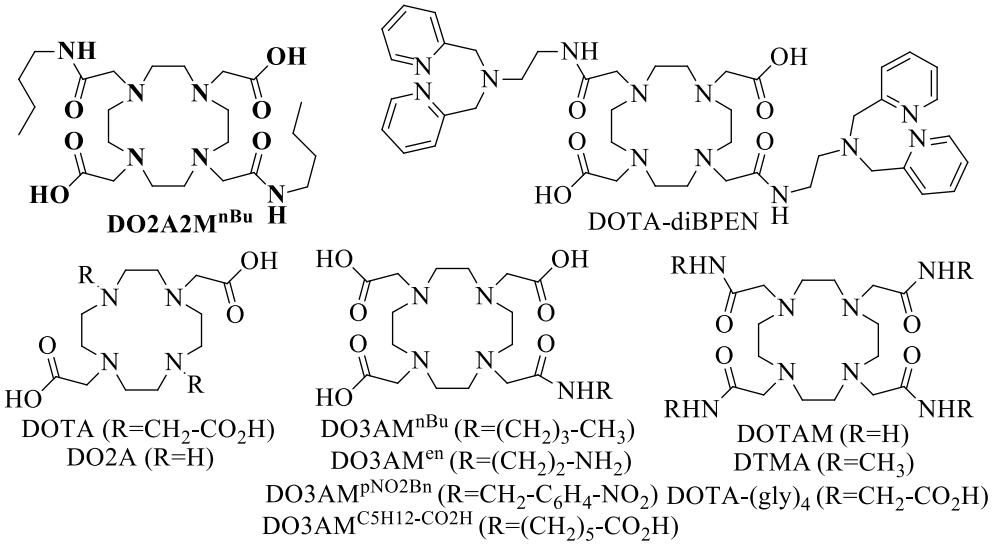

Fig. 1. Structure of DOTA and some amide derivatives.

DOTA to a biological vector, one of the four carboxylate groups is often modified to form a substituted amide. A number of DOTA-monoamide derivatives have been prepared and their Gd(III) complexes used as the basic design of a responsive CA for detection of biomarkers such as extracellular pH or for attachment to a specific targeting molecule [10–15]. The thermodynamic stability of the GdDO3A-monoamide complexes is somewhat lower than $[Gd(DOTA)]^-$ because the Gd(III)-amide oxygen bond is weaker than a Gd(III)-carboxylate oxygen bond [16–18]. The substitution of amides for all four carboxylate groups of DOTA affords DOTA-tetra(amide) ligands such as DOTAM (1,4,7,10-tetrakis(carbamoylmethyl)-1,4,7,10-tetraazacyclododecane) and DTMA (1,4,7,10-tetra(methylcarbamoylmethyl)-1,4,7,10-tetra-azacyclodoecane) (Fig. 1). These ligands form Ln(III) complexes with lower thermodynamic stability but the resulting complexes remain reasonably kinetically inert as their dissociation rates are comparable to those of the $Ln(DOTA)^-$ complexes [19,20]. This feature makes them attractive candidates for certain selective applications. For example, the positively charged complexes, $Ln(DOTAM)^{3+}$ and $Ln(DTMA)^{3+}$, have been use to catalyze cleavage of ribonucleic acid (RNA) oligomers [21].

DOTA forms complexes with the Ln(III) ions by occupying eight coordination sites on the metal ion in either a square antiprism (SAP) or twisted square antiprism geometry (TSAP) geometry with a water molecule coordinated to the Ln(III) ion in a capping position. In $Gd(DOTA)(H_2O)^-$, this water molecule exchanges rapidly with the surrounding water molecules and transfers the paramagnetic relaxation effects of Gd(III) into the bulk water pool of protons. The net result of this exchange is an increase in proton relaxation rates, both R_1 and R_2. This relaxation rate, expressed as r_{ip} (i = 1, 2) relaxivity (referenced to the proton relaxation rate of a sample containing 1 mM paramagnetic agent), strongly depends on the rate of water molecule exchange between the inner-sphere of the Gd(III) complex and bulk water. The replacement of only one carboxylate group on DOTA with an amide alters the water exchange rate only slightly (by a factor 3 in case of $DO3AM^{nBu}$ and $DO3AM^{pNO2Bn}$ or by a factor of 5 in case of $DO3AM^{C5H10-CO2H}$) [5,15,22] but if all the carboxylates are replaced by amides, the rate of water exchange in $Eu(DOTA(gly)_4)^-$ ($DOTA(gly)_4$ is the tetra-glycinate amide of DOTA = 1,4,7,10-tetraazacyclododecane-1,4,7,10-tetrakis(acetamidoacetic acid)) [23] is more than three orders of magnitude slower than that in $Gd(DOTA)(H_2O)^-$ [5]. Given this surprisingly low rate of water exchange, it was quickly recognized that the DOTA-tetraamide complexes of Eu(III), Dy(III), Tm(III) and Yb(III) might be used as paramagnetic chemical exchange saturation transfer (paraCEST) agents in which the slowly exchanging inner-sphere water molecule and the amide –NH protons can be selectively saturated to generate different CEST effects [5,24,25].

A few $GdDOTA-(amide)_2$ derivatives having *trans*-acetate and -amide groups have been recently reported as responsive agents for detection of Zn^{2+} ions in vivo [26–29]. The amide groups in these systems each have a highly selective Zn^{2+} binding unit, *N*,*N*-bis(2-pyridyl-methyl)ethylene diamine (di-(2-picolyl)amine, DPA) which upon binding of Zn^{2+} then form a ternary complex with human serum albumin (HSA). This results in slower molecular rotation of the entire Gd(III) complex and consequently a remarkable increase in r_1 relaxivity. This mechanism allows the agent to highlight or brighten only those tissues that secrete Zn^{2+} ions in response to a biological event such as an increase in plasma glucose. So far, these Zn^{2+} responsive agents have been used to image beta-cell function and prostate cancer in animal models by MRI [26,29].

The structure, luminescence and relaxation properties of the Ln(III) complexes of the DO2A-bisamide type ligands and some potential biological applications have been reported to the literature [30,31]. Very recently T. J. Sorensen and co-workers have studied the structure and luminescence properties of Eu(III) and Yb(III) complexes formed with a large variety of cyclen based chelators (DOTA-mono-, di- and tetra(amide)s as well as some DO3A-derivatives) [31], including a DO2A-bis(amide) type ligand, but there is relatively scarce information on the stability and kinetic properties of these complexes. To obtain more fundamental information about the effects of acetate-to-amide substitution in complexes of this type, we prepared $DO2A2M^{nBu}$ (Fig. 1) as a model compound and studied the thermodynamic and kinetic properties of complexes formed with Mg^{2+}, Ca^{2+}, Zn^{2+}, Cu^{2+} and some Ln(III) ions.

2. Results and discussion

2.1. Synthesis of the macrocyclic ligands

The synthetic scheme for preparation of $DO2A2M^{nBu}$ is shown in Scheme 1. The starting material 1,4,7,10-tetraazacyclodoecane-1,7-di (acetic acid tert-butyl ester) (DO2A-tert-butyl ester) (**1**) prepared by published methods was alkylated with *N*-(butyl)-2-bromoacetamide (**2**). Hydrolysis of the tert-butyl ester intermediate (**3**) in dichloromethane with trifluoroacetic acid (TFA) followed by repeated lyophilization form diluted HCl solution afforded the desired final product 1,4,7,10-tetraazacyclodoecane-1,7-di(acetic acid)-4,10-di(*N*-butylacetamide) ($DO2A2M^{nBu}$) (**4**) as dihydrochloride salt.

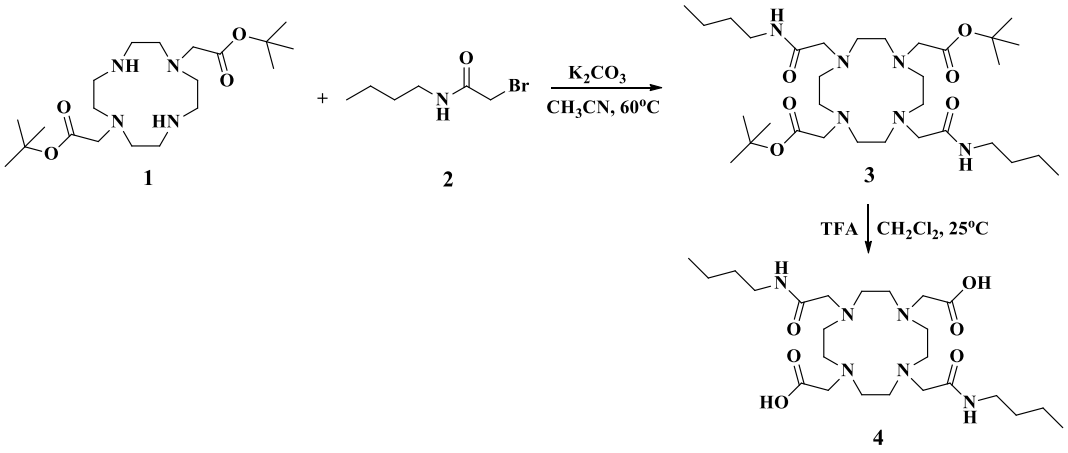

Scheme 1. Synthesis of 1,4,7,10-tetraazacyclodoecane-1,7-di(acetic acid)-4,10-di(*N*-butylacetamide) ($DO2A2M^{nBu}$).

2.2. Equilibrium studies

The complexation properties of $DO2A2M^{nBu}$ are expected to be different from DOTA due to the presence of the two butyl-amide groups. To evaluate these differences, the stability constants of the complexes formed between $DO2A2M^{nBu}$ and some biologically important metal ions (Mg^{2+}, Ca^{2+}, Zn^{2+}, Cu^{2+}) and lanthanide ions were determined. Given that the kinetic inertness of the Ln(III) complexes is an important consideration for in vivo safety, the formation and dissociation kinetics of some $Ln(DO2A2M^{nBu})^{+}$ complexes were also examined.

2.3. Stability constants

The protonation constants of the ligand $DO2A2M^{nBu}$, determined by pH potentiometric titrations, are listed in Table 1 as log K_i^H values (the calculated standard deviation values are given in parenthesis while their definitions were included in the ESI). The protonation constants of DOTA, $DO3AM^{nBu}$ ($DO3AM^{nBu}$ = 1,4,7,10-tetraazacyclodoecane-1,7-di (acetic acid) -(*N*-butylacetamide)) DO2A (DO2A = 1,4,7,10-tetraazacyclodoecane-1,7-di(acetic acid)) and DTMA are also listed for comparison purposes.

Table 1
Protonation constants of ligands and stability constants of complexes formed with Mg^{2+}, Ca^{2+}, Zn^{2+} and Cu^{2+} ions (25 °C, 1.0 M KCl).

	DOTA[a]	$DO3AM^{nBu}$, [b]	$DO2A2M^{nBu}$, [c]	DO2A[e]	DTMA[f]
log K_1^H	11.9	10.17	10.31(1); 8.31(4)[d]	10.91	9.56
log K_2^H	9.72	9.02	9.04(1); 8.57(1)[d]	9.45	5.95
log K_3^H	4.60	4.41	2.86(2); 3.06(2)[d]	4.09	–
log K_4^H	4.13	2.94	2.21(3); 2.22(2)[d]	3.18	–
log K_5^H	2.36	1.99	1.93(4)	–	–
MgL	11.85	–	8.30(1)	5.40	4.33
MgHL	–	–	5.78(4)	–	–
CaL	17.2	–	13.29(1)	7.8[g]; 7.16[h]	10.1
CaHL	3.7	–	3.56(5)	–	–
ZnL	20.8	–	17.67(4)	18.2[g]	13.66
ZnHL	4.24	–	3.21(2)	4.0	–
$ZnHL_{-1}$	–	–	5.83(6)	–	10.71
CuL	21.98[i]	–	19.59(2)[d, j]	21.17	14.61
CuHL	4.08[i]	–	2.67(1)[d, j]	3.0	–
CuH_2L	3.41[i]	–	1.77(1)[d, j]	–	–
$CuHL_{-1}$	–	–	11.64 (3)[d, j]	–	8.78[k]

[a] Ref. [32].
[b] Ref. [15].
[c] This work.
[d] Determined by using 1.0 M NaCl ionic background.
[e] Ref. [33].
[f] Ref. [20].
[g] Ref. [34].
[h] Ref. [35].
[i] logK_{CuH3L} = 0.83 and log K_{Cu2L} = 2.42 were also published in 0.15 M NaCl.
[j] Determined by simultaneous fitting of pH-potentiometric and UV–vis spectrophotometric data (ESI Fig. S1) by using 1.0 NaCl as the ionic strength.
[k] A second deprotonation step was also detected in the $Cu(DTMA)^{2+}$ complex [20].

The data listed in Table 1 show that the protonation constants of DOTA-amide derivatives generally decrease with each successive replacement of a DOTA carboxylate group with an amide. This reflects loss of charge stabilization provided by ionic interaction between a protonated macrocyclic amine and a deprotonated carboxyl group on acetate attached to that amine [36]. The microscopic protonation steps in DOTA and its derivatives have been previously determined by ^1H and ^{13}C NMR spectroscopy [37,38] and on the basis of those previous observations, the protonation sites in $DO2A2M^{nBu}$ are easily predicted. The first and second protonation steps occur on the two trans-macrocyclic nitrogen atoms that carry the acetate groups, stabilized by charge interactions between the protonated nitrogen atoms and the negatively charged carboxylate groups. The log K_3^H and log K_4^H values of the $DO2A2M^{nBu}$ are much lower than those of the DOTA (Table 1) because the third and fourth protonation steps likely occur at the two carboxylate groups involved in charged interactions with the protonated amines.

The stability constants of complexes formed with divalent M^{2+} metal ions are also presented in Table 1. The stability of the Mg^{2+}, Ca^{2+} and Zn^{2+} complexes were determined by direct pH-potentiometric titration whereas UV–vis spectrophotometric titrations performed for the Cu^{2+} complex over the acid concentration range of 0.01–1.00 M (ESI Fig. S1). It was found that the log K_{ML} values decrease with an increase in number of amide groups, consistent with a stronger interaction of the M^{2+} metal ions with the carboxylate donor atoms than with the amide oxygen atoms (for the Gd(III) ion it was evidenced by calculating the pGd values for the representative complexes vide infra). While Mg^{2+} and Ca^{2+} ions form more stable complexes with the octadentate $DO2A2M^{nBu}$ than with the hexadentate DO2A, the log K_{ML} values of Zn^{2+} and Cu^{2+} complexes with these same two ligands are similar, likely reflecting a lower coordination number of six for both Zn^{2+} and Cu^{2+} (as observed for Cu^{2+} in $CuH_2(DOTA)$ and $Cu_2(DOTA)$ complexes [39,40] by X-ray crystallography in the solid state). In these two complexes, the two amide groups in $DO2A2M^{nBu}$ would not be expected to participate in metal ion binding. It is also interesting to note that protonation of the $M(DO2A2M^{nBu})$ complexes to form the MHL species is more difficult (lower MHL constants) for those complexes of greatest stability (Cu^{2+} > Zn^{2+} > Ca^{2+} > Mg^{2+}). This indicates that protonation of the ML complexes occurs at carboxylate groups which are already coordinated to the metal ion.

The stability constants of the lanthanide $DO2A2M^{nBu}$ complexes are

Table 2
Stability constants (log K_{ML}) of the lanthanide(III) complexes (I = 1.0 M KCl, 25 °C).

Complex	DOTA[a]	DO3AM^{nBu}[b]	DO2A2M^{nBu}[c]	DTMA[d]	DO2A[e]
CeL	23.39	19.26	16.98 (8)	12.68	11.31
NdL	22.99	–	18.71 (7)	13.08	12.56
EuL	23.45	–	19.32 (9)	13.67	12.99
GdL	24.67	21.29	19.30 (9)	13.58	13.06
pGd[f]	18.86	17.87	15.72	12.39	8.44
HoL	24.54	–	19.64 (8)	13.84	13.00
YbL	25.00	–	19.36 (9)	–	13.26
LuL	25.41	21.83	19.49 (8)	13.91	13.16

[a] 0.1 M NaCl, 25 °C Ref. [42].
[b] Ref. [15].
[c] This work.
[d] 1.0 M KCl, 25 °C Ref. [20].
[e] Ref. [35, 43].
[f] Calculated by using the following conditions: c_{lig} = 10 μM, c_{Gd} = 1 μM and pH = 7.4.

presented in Table 2 along with some comparative values for other DOTA-derivatives. The stability of the Ln complexes (log K_{ML}) follow the same trend as observed for the complexes of divalent M^{2+} metal ions, i.e., the log K_{ML} values decrease in proportion with the number of amide groups in the ligand. These log K_{ML} data also indicate that the Ln^{3+}-amide oxygen bonds are weaker than the Ln(III)-carboxylate oxygen bonds. The stability constants of the Ln(DO2A2M^{nBu})$^{+}$ complexes are approximately six log K units larger than those of the Ln(DO2A)$^{+}$ complexes, indicating that the coordination of each amide group improves the stability of Ln(III) complexes by about three log K units. This gain in the stability due to the coordination of an amide group is very close to the value (3.38 log K unit) previously predicted for the increase in stability constants per an additional coordinating amide moiety [41].

The stability constants of Ln(III) complexes of DOTA-amide ligands show a similar trend as the Ln(DOTA)$^{-}$ chelates along the lanthanide series with log K_{ML} values increasing from Ce(III) to Eu(III)/Gd(III) then only modest changes for the heavier lanthanide metals. This observation is assumed to reflect best fit of the medium size ions (Eu(III), Gd(III)) into the coordination cage formed by the nitrogen and oxygen donor atoms of the ligands.

2.4. Kinetics of complex formation

Metal ion complexes of DOTA and DOTA-derivatives have the metal ion in the center of coordination cage formed by the four ring nitrogen atoms and up to four donor atoms from the pendant functional groups (carboxylate and amide oxygen atoms etc.). Entry of a tripositive Ln(III) ion into the cage is generally slow because the donor atoms of the functional groups, particularly the negatively charged carboxylate oxygens, form an intermediate complex with the metal ion outside the cage and this intermediate complex slows movement of the ion into the final coordination cage. Over the pH range of 3–7 where the complexation of Ln(III) ions is typically studied, two macrocyclic ring nitrogen atoms are protonated and the repulsion of these positive charges with the entering Ln(III) also slows complex formation. These protons must first be removed from the intermediate "uncaged" complex for the metal ion to enter into the coordination cage [44–46]. The presence of the negatively charged carboxylate groups in DOTA is also very important for formation of the "uncaged" intermediates because, in the absence of such charged groups, the mechanism of complex formation proceeds by a completely different mechanism. Simple DOTA-tetra(amides) such as DOTAM and DTMA do not have negatively charged functional groups, so these ligands cannot form stable intermediates [23]. Detailed kinetic studies have shown that the Ln(DOTAM)$^{3+}$ and Ln(DTMA)$^{3+}$ complexes form by direct reaction between the Ln^{3+} ion and the fully deprotonated ligand [20,47]. It is worth noting however, that in case of DOTA-(gly)$_4$, a ligand with extended carboxylate side-arms, a complex formation mechanism (more detailed information about the mechnaism of Ln^{3+} complex formation is given in the ESI) similar to that observed for the Ln(DOTA)$^{-}$ chelates was observed [19].

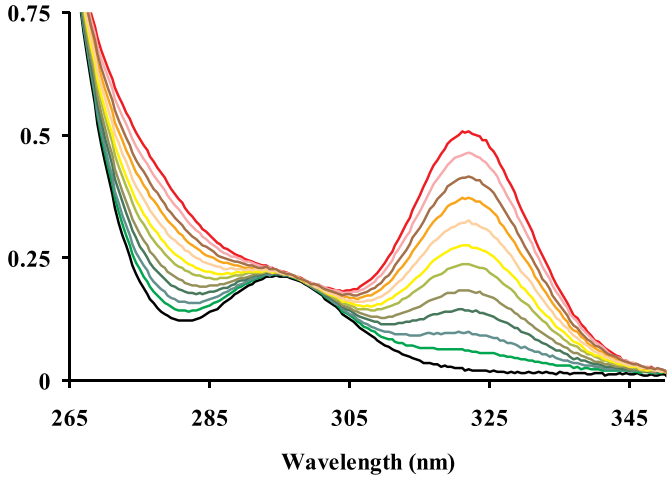

Fig. 2. Absorption spectra of $CeCl_3$ plus DO2A2M^{nBu} at different times after mixing (c_{Ce} = 5.0 mM; c_{lig} = 1.0 mM; 25 °C; pH = 4.66). The black line in the spectrum was recorded immediately after mixing (1 min), while the others correspond to the following time points: 26, 51, 86, 121, 176, 226, 301, 401, 526, 751 min after mixing and at equilibrium (red) from bottom to top.

To examine the mechanism of complex formation in a mixed side-chain ligand, the formation rates of the Ln(DO2A2M^{nBu})$^{+}$ complexes (Ln(III) = Ce(III), Eu(III) and Yb(III)) were studied by spectrophotometry. UV–vis spectra of Ce(III) plus DO2A2M^{nBu} immediately after mixing shows an absorption maximum at 295 nm (Fig. 2), a peak characteristic of the aqueous Ce(III) ion. A peak characteristic of an uncaged intermediate was not detected, similar to the spectra observed during the formation of the Ln(DOTA-(gly)$_4$)$^{-}$ complexes [23]. The progress of the reaction is indicated by a gradual increase in an absorption maximum at 322 nm characteristic of formation of the final caged complex, Ce(DO2A2M^{nBu})$^{+}$. The rates of complex formation were studied further by following the absorbance values at 322 nm at different Ce(III) concentrations and solution pH. The concentration of Ce(III) in the samples was 10–40 times higher than that of the DO2A2M^{nBu} to ensure pseudo-first-order conditions for analysis of the kinetic data.

Under such conditions, the rate of complex formation can be expressed as follows (Eq. (1)):

$$\frac{d[\mathrm{LnL}]_t}{\mathrm{dt}} = k_{\mathrm{obs}}[\mathrm{L}]_t \quad (1)$$

where $[L]_t$ and $[LnL]_t$ are the total ligand and complex concentrations at time t, while k_{obs} is a pseudo-first-order rate constant characterizing the rate of complex formation. The k_{obs} values determined at different Ce(III) concentrations and pH values are presented in Fig. 3. The dependence of the complex formation rates on the Ce(III) concentrations follow saturation behavior. This indicates that rapid formation of an intermediate and slow formation of the final complex involves loss of proton(s) and concomitant rearrangement of the intermediate to the fully formed complex [48].

The formation rates of Eu(DO2A2M^{nBu})$^{+}$ were also studied by monitoring the charge-transfer band of the complex at 250 nm by UV–vis spectrophotometry, where the absorption of $Eu(III)_{aq}$ ion is negligible. The k_{obs} values determined at different Eu(III) concentrations and pH values are shown in Fig. 4. The k_{obs} values also show saturation behavior with increasing Eu(III) concentration.

The formation rates of Yb(DO2A2M^{nBu})$^{+}$ complex was studied by

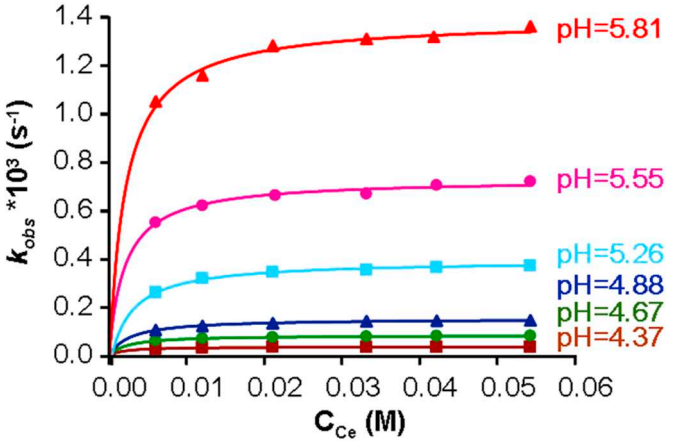

Fig. 3. Pseudo-first-order rate constants, k_{obs}, for the formation of Ce(DO2A2M^{nBu})$^+$ complex. c_{lig} = 0.5 mM; pH = 4.37, 4.67, 4.88, 5.26, 5.55 and 5.81 going upwards.

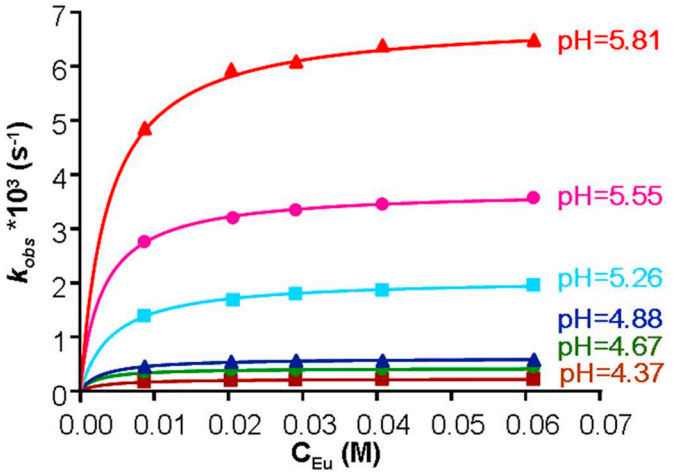

Fig. 4. Pseudo-first-order rate constants, k_{obs}, for the formation of Eu(DO2A2M^{nBu})$^+$. c_{lig} = 0,5 mM; pH = 4.37, 4.67, 4.88, 5.26, 5.55 and 5.81 going upwards.

the "indicator method" since none of the reactants (Yb(III) and the DO2A2M^{nBu} ligand) or the product of the reaction (the Yb(DO2A2M^{nBu})$^+$ complex) possess an absorption band in the UV or vis range of the electromagnetic spectrum [49]. The measured pseudo-first-order rate constants, k_{obs}, for the formation of Yb(DO2A2M^{nBu})$^+$ are presented as a function of Yb^{3+} concentration in the ESI (Fig. S2).

The saturation curves in Figs. 3–4 and S2 show that the complex formation rates depend on the Ln^{3+} ion concentration. These curves can be described by Eq. (2) [48]:

$$k_{obs} = \frac{k_f K_C^* [Ln^{3+}]}{1 + K_C^* [Ln^{3+}]} \quad (2)$$

where K_C^* is the conditional stability of the intermediate and k_f is the rate constant for the complex formation when the intermediate formation is complete (at the saturation of the curves K_C^*[Ln(III)] ≫ 1 and $k_{obs} = k_f$). The k_f and K_C^* values were calculated by fitting the k_{obs} values to Eq. (2). The experiments were performed in the pH range 4–6 where the ligand is present in the form of H_2L, H_3L, H_4L and H_5L protonated species so the stability of the diprotonated intermediate K^*(Ln(H_2L))* detected during formation of Ln(DOTA), other LnDOTA-derivative complexes, and Ln(DO2A) [44–46,50] can also be calculated from these kinetic data. K^* = [Ln(H_2L)] / [Ln(III)] [H_2L] can be calculated by use of K_C^* conditional stability constants determined in the kinetic studies as follows: $K^* = \alpha_H * K_C^*$, where $\alpha_H = 1 + K_3^H [H^+] + K_3^H K_4^H [H^+]^2 + K_3^H K_4^H K_5^H [H^+]^3$. The resulting calculated K^* stability constants characterizing the extent of formation of a reaction intermediate are presented in Table 3.

Table 3
Formation rate constants (k_{OH}, $M^{-1}s^{-1}$) for several Ln(DOTA)$^-$ and DOTA-type complexes and the stability constants of the reaction intermediates (K^*).

Ligand	Ce(III)	Eu(III)	Yb(III)
DOTA[a]	3.5×10^6	1.1×10^7	4.1×10^7
DO3AM^{en}, [b]	9.7×10^5	1.7×10^7	–
DO2A[c]	2.8×10^5	–	2.5×10^5
DO2A2M^{nBu}, [d]	$1.33(6) \times 10^5$	$6.6(3) \times 10^5$	$1.18(3) \times 10^7$
DOTAM[e, f]	7.7×10^3	2.7×10^4	6.6×10^3
DTMA[f, g]	3.0×10^4	4.8×10^4	6.5×10^3
log K^*(Ln(H_2DOTA)$^+$)[h]	7.61 (La); 4.5[i]	7.25 (Gd); 4.3[i]	7.46 (Lu); 4.2[i]
log K^*(Ln(H_3DO3AM^{en})$^{3+}$)[b]	4.91 (La)	4.89 (Gd)	4.44 (Lu)
log K^*(Ln(H_2DO2A)$^{3+}$)[c]	1.98	–	1.60
log K^* (Ln(H_2DO2A2M^{nBu})$^+$)[d]	2.66 ± 0.05	2.47 ± 0.07	1.26 ± 0.04

[a] The formation of Ln(DTMA)$^{3+}$ and Ln(DOTAM)$^{3+}$ complexes is a second order reaction (k: $M^{-2}s^{-1}$) between the Ln(III) ion and deprotonated ligand.
[b] Ref. [44].
[c] Ref. [18].
[d] Ref. [50].
[e] This work.
[f] Ref. [47].
[g] Ref [20].
[h] Ref [53] determined by pH-potentiometric method.
[i] Ref. [44] determined by UV–vis method form kinetic data.

The rate constants k_f characterizing the formation of the Ce(III), Eu(III) and Yb(III) complexes at different pH values are presented in Fig. 5 as a function of OH^- concentration. The data in Fig. 5 show that the k_f rate constants are proportional to the OH^- concentration i.e. $k_f = k_{OH}$ [OH^-]. This very simple rate law is similar to those observed for the complex formation reactions of DOTA and other DOTA derivatives [44,46,50–52]. The formation of Ln(III) complexes is a general base-catalyzed reaction (the catalyst is OH^- or any other base present in the sample). The validity of a base-catalyzed mechanism for the formation of the Ln(DO2A2M^{nBu})$^+$ complexes was confirmed by studying the rates of formation reactions at constant pH by varying the concentration of the buffer (see details in the ESI, Fig. S3). The calculated k_{OH} values are listed in Table 3 where some data for the formation of other DOTA-amide derivative complexes are also shown for comparison.

The comparison of the k_{OH} rate constants in Table 3 generally shows a similar trend that was observed for the formation of Ln(DOTA)$^-$ complexes. The k_{OH} values increase with the decrease of the ionic size of Ln(III) ions likely reflecting a decrease in stability of the

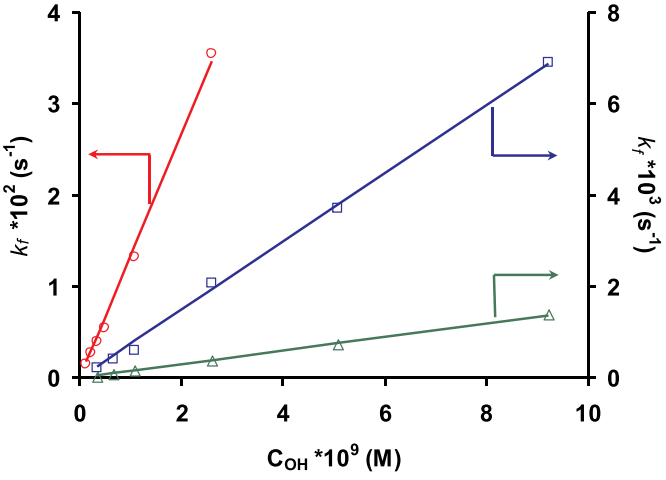

Fig. 5. Formation rates of the Ln(DO2A2M^{nBu}) complexes (Ln = Ce (green), Eu (blue), Yb (red), 25 °C, 1.0 M KCl).

intermediates from Ce(III) to Yb(III) [44,50]. The replacement of the carboxylates with amide groups only slightly diminishes the formation rates of complexes, even though this substitution appears to strongly affect the stability of intermediates.

The linear increase of the formation rates of complexes with increasing OH^- concentration suggests OH^- catalyzed deprotonation of the $Ln(H_2L)^*$ intermediates, but the interpretation of experimental data is somewhat more complicated. Detailed studies have shown that a dissociation equilibrium exists between the $Ln(H_2L)^*$ and $Ln(HL)^*$ intermediates ($Ln(H_2L)^* \rightleftarrows Ln(HL)^* + H^+$). It is well known that the rate determining step of complexation is the loss of proton from the monoprotonated intermediate [46]. However, the concentration of the $Ln(HL)^*$ intermediate is directly proportional to $1/[H^+]$ because of the dissociation equilibrium [45,46]. The $1/[H^+]$ dependence of the formation rates can be simply described as a dependence on OH^- concentration, so the k_{OH} rate constants can be conveniently used for comparison. The formation rate constants of DOTA-mono(amide) and -bis(amide) complexes in Table 3 cannot be directly compared with the rate constants characterizing the formation rates of the $Ln(DOTAM)^{3+}$ and $Ln(DTMA)^{3+}$ complexes because the formation of these complexes does not involve protonated intermediates. The formation rate constants, k_{OH}, gradually increase from Ce(III) to Eu(III) and to Yb(III) for all three $Ln(DOTA)^-$, $Ln(DO3AM^{en})$ and $Ln(DO2A2M^{nBu})^+$ complexes. This trend is the opposite to the variation of the water exchange rate on the Ln(III) aqua ions along the lanthanide series, which decreases from $k_{ex}^{298} = 83$ to $4.7 \times 10^7\ s^{-1}$ between Gd(III) and Yb(III), while the water exchange mechanism remains associatively activated [54]. Therefore, one can conclude that water exchange has no implication in the formation reaction. Conversely, the water exchange could play a role in the formation reactions of the $Ln(DOTAM)^{3+}$ and $Ln(DTMA)^{3+}$ complexes because the rates of both the complex formation and the water exchange follow the same trend, they increase along the lanthanide series [20,47].

2.5. Kinetic inertness of some representative $Ln(DO2A2M^{nBu})^+$ complexes

The kinetic inertness of a lanthanide(III) complex is an important requirement for their use in diagnostic medicine because both the Ln(III) ions and the aminopolycarboxylate ligands formed by dissociation are known to be toxic, although the ligand is known to have a less pronounced impact. Previous studies have demonstrated the high kinetic inertness of many Ln(DOTA) and LnDOTA-derivative complexes [44,50,51,55–57]. These studies have also indicated that the transmetallation reactions of the Ln(DOTA) type complexes with biological ions such as Cu^{2+} and Zn^{2+} do not take place directly via an associative pathway but rather occur after proton or endogenous ligand assisted dissociation of the complexes [44,50,55,56]. Proton assisted dissociation of the Ln(DOTA) type complexes is very slow at physiological pH values so dissociation rates can be conveniently studied only in acidic solutions (e.g. in 0.1 M HCl [56]) where the complexes are thermodynamically unstable and their dissociation is quantitative. Accordingly, the dissociation rates of $Ce(DO2A2M^{nBu})^+$ and $Eu(DO2A2M^{nBu})^+$ were studied by spectrophotometry in the 0.2 M – 2.0 M HCl concentration range by maintaining constant ionic strength with the addition of NaCl keeping the sum of the HCl and NaCl concentrations at 3.0 M. The concentration of complexes was significantly lower (1.0 and 2.0 mM for Ce and Eu complexes, respectively) than the H^+ concentration so the dissociation reactions could be regarded as kinetically pseudo-first-order and the rate of dissociation of complexes could be expressed by the Eq. (3):

$$-\frac{d[LnL]_t}{dt} = k_d[LnL]_t \quad (3)$$

where $[LnL]_t$ is the total concentration of the complex and k_d is the pseudo-first-order rate constant. The k_d first-order dissociation rate constants, obtained from plots such as those shown in Fig. 6, increase linearly with increasing H^+ concentration and the dependence of k_d values on the $[H^+]$ can be expressed by Eq. (4):

$$k_d = k_0 + k_1[H^+] \quad (4)$$

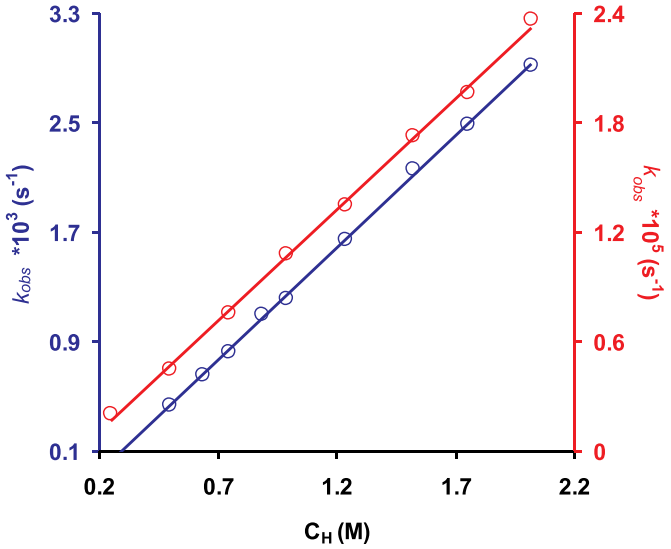

Fig. 6. Dependence of the rate of acid catalyzed dissociation of $Ln(DO2A2M^{nBu})^+$ complexes as a function of H^+ ion concentration ($Ce(DO2A2M^{nBu})^+$ - blue; $Eu(DO2A2M^{nBu})^+$ - red).

In Eq. (4) the k_0 and k_1 rate constants characterize the spontaneous and proton assisted dissociation rates of the complexes, respectively. The k_0 values were found to be very small and the calculated errors were relatively high, which indicates that the spontaneous dissociation of $Ce(DO2A2M^{nBu})^+$ and $Eu(DO2A2M^{nBu})^+$ is negligible. The dissociation rates of the DOTA and DOTA derivative complexes can generally be described by the Eq. (4), so the k_0 and k_1 values listed in Table 4 can be used to compare the kinetic behavior of complexes. It should be noted that spontaneous dissociation (k_0 values) plays an important role in the dissociation of Ln(DOTA-tetra(amide)) complexes.

The comparison of the k_1 rate constants presented in Table 4 shows that, like the stability constants (Table 2), the kinetic inertness of the complexes also increases from the from Ce(III) to Eu(III) (the rates of proton assisted dissociation decrease in the order of Ce(III) > Eu (III) > Yb(III)). However, while the stability constants gradually decrease with the successive substitution of amides for the carboxylates of DOTA, the k_1 rate constants are not affected appreciably by the replacement of one or two carboxylate groups.

Mechanistically, the acid catalyzed dissociation of these complexes starts with the protonation at a non-coordinated carboxylate oxygen atom. In order for the complex to dissociate, the proton must be transferred to a ring nitrogen so that the Ln(III) can move out of the coordination cage as a result of the electrostatic repulsion between the protonated nitrogen and the Ln(III) ion. The complexes of the DO3A-mono(amide) and DO2A-bis(amide) ligands possess carboxylate groups that can be protonated, so the presence of 1–2 amide group(s) in the ligands does not significantly hinder the protonation and proton assisted dissociation of the complex and, consequently, the dissociation rate of these complexes is similar to that of the corresponding Ln $(DOTA)^-$ complexes. The situation is different for the $Ln(DOTAM)^+$ and $Ln(DTMA)^+$ complexes because the electrostatic interaction between the Ln^{3+} ion and neutral ligand is weaker so spontaneous dissociation becomes more likely even though proton assisted dissociation (k_1) is slower compared to the $Ln(DOTA)^-$ complexes due to the low basicity of the amide oxygen atoms. The relatively high rate of spontaneous dissociation of $Ce(DTMA)^{3+}$ ($k_0 = 1.1 \times 10^{-5}\ s^{-1}$) governs the 17.5 h dissociation half life ($t_{1/2} = \ln_2/k_0$) independent of the pH while the proton assisted dissociation of this complex is very slow at

Table 4
Rate constants, k_0 and k_1, that characterize dissociation of the Ln(III)-DOTA-amide complexes.

Ln		DOTA	DO3AM[en, e]	DO2A2M[nBu, f]	DTMA[g]
Ce(III)	k_0 (s^{-1})	–	–	–	1.1×10^{-5}
	k_1 ($M^{-1}s^{-1}$)	3.3×10^{-4}, [a]	–	$1.64(4) \times 10^{-3}$	2.6×10^{-5}
Eu(III)	k_0 (s^{-1})	–	–	–	1.5×10^{-7}
	k_1 ($M^{-1}s^{-1}$)	1.4×10^{-5}, [b]	–	$1.22(6) \times 10^{-5}$	5.6×10^{-7}
Yb(III)	k_0 (s^{-1})	6.7×10^{-11}, [c]	–	–	–
	k_1 ($M^{-1}s^{-1}$)	8.4×10^{-6}, [d]; 1.8×10^{-6}, [c]	2.6×10^{-6}	–	–

[a] Ref. [57].
[b] Ref. [44].
[c] Ref. [55].
[d] Ref. [18].
[e] Ref. [51].
[f] This work.
[g] Ref. [20].

physiological pH values ($t_{1/2} = 1.85 \times 10^8$ h). These data show that spontaneous dissociation can significantly diminish the kinetic inertness of the positively charged LnDOTAM-like complexes. However, this pathway was found not to contribute significantly to the dissociation of the Ln(III) complexes of tetra-amide ligands having charged groups such as DOTA-$(gly)_4$ [23].

The thermodynamic and kinetic studies in this work clearly demonstrate the high thermodynamic stability and kinetic inertness of the $Ln(DO2A2M^{nBu})^+$ complexes. It was also shown that these complexes have negligible spontaneous and very slow proton assisted dissociation making them suitable candidates for biological applications such as those recently reported for the detection of Zn^{2+} ions by MRI [27–30].

2.6. The rate of water exchange in $Gd(DO2A2M^{nBu})^+$

The kinetics of water exchange is an important property for Gd-complexes used as MRI contrast agents. Indeed, the paramagnetic effect of the metal ion is transmitted to bulk via the exchange of typically a single inner-sphere coordinated molecule and bulk water. This solvent exchange can be neither too slow nor too fast in order to observe efficient nuclear relaxation of bulk water protons. In the last decades, the rates and mechanisms of water exchange have been assessed in a large number of Gd-complexes, including many derivatives of $Gd(DOTA)^-$. It has been established that most of these complexes undergo water exchange via a dissociative mechanism and that replacement of carboxylates by amides results in slower water exchange rates.

To compare water exchange rates for $Gd(DO2A2M^{nBu})^+$ with previously published values, a variable temperature ^{17}O NMR study was performed to measure the ^{17}O transverse (■) and longitudinal (▲) relaxation rates ($1/T_2$ and $1/T_1$) and chemical shifts (♦) on an aqueous solution of the complex (Fig. 7). The paramagnetic contribution to the transverse and the longitudinal relaxation rates were determined as the difference between $1/T_{1,2}$ values of the $Gd(DO2A2M^{nBu})^+$ and a reference sample (acidified water). As shown in Fig. 7, the reduced transverse relaxation rates decrease with decreasing temperature over most of the temperature range studied (275–350 K). This corresponds to a slow water exchange system. Similarly, the chemical shift (Δω) approaches zero as the sample is cooled, also consistent with relatively slow water exchange. Under these conditions, no information can be obtained from the chemical shift values about the number of inner sphere water molecules. On the other hand, the transverse relaxation rates are almost exclusively dependent on the water exchange rate, therefore the exchange rate can be determined with good confidence.

The relaxation rates and the chemical shifts were analyzed using standard Solomon-Bloembergen-Morgan theory of paramagnetic relaxation (the equations are included in the ESI). In this analysis, the hydration number was fixed at 1 based on similar complexes. The following parameters were fitted to these data: k_{ex}^{298}, the activation

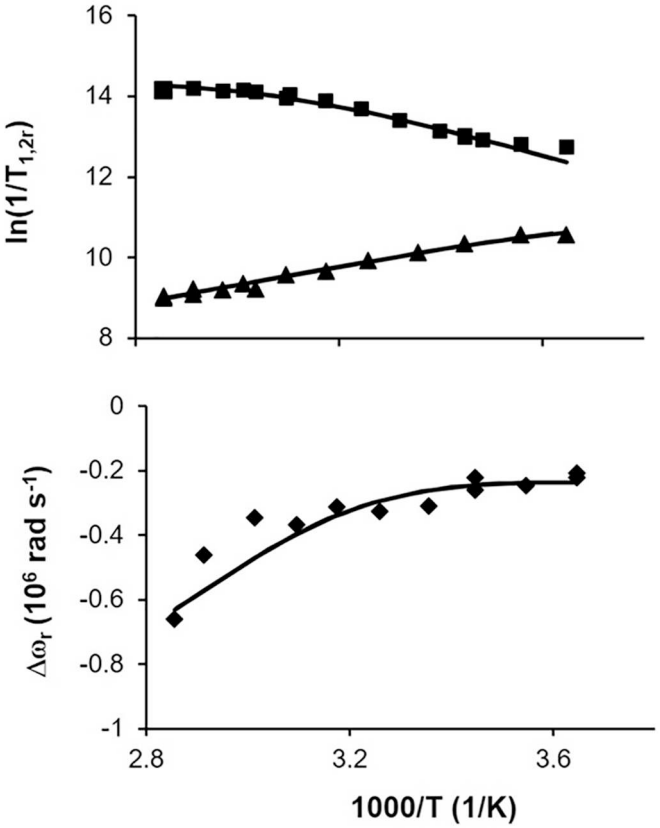

Fig. 7. Temperature dependence of the reduced transverse $1/T_{2r}$ (■) and longitudinal $1/T_{1r}$ (▲) ^{17}O relaxation rates, and the reduced ^{17}O chemical shifts, $\Delta\omega_r$ (♦) for $Gd(DO2A2M^{nBu})^+$. The curves represent the best fit to the experimental data as described in the text.

enthalpy $\Delta H^{\ddagger}$ and entropy $\Delta S^{\ddagger}$ of the water exchange, the rotational correlation time τ_R^{298} and activation energy, E_R. Also included in the fit was an empirical constant describing the outer sphere contribution to the chemical shifts, C_{os}, and the parameters describing the electron spin relaxation, τ_v^{298} and Δ^2, the correlation time for the modulation of the zero field splitting and the energy of zero field splitting. However, these electronic relaxation parameters are determined with poor accuracy because the slow exchange regime T_2 depends only on the water exchange rate and electron spin relaxation has a role only at the highest temperatures. Other parameters were fixed to typical values, such as the scalar coupling constant $A/\hbar = -3.8$ MHz, the distance between the Gd and the coordinated water oxygen, $r_{GdO} = 2.5$ Å, and the

Table 5
Parameters obtained for Gd(DO2A2M^{nBu})$^{+}$ from the fitting of the transverse and longitudinal ^{17}O NMR relaxation rates and chemical shifts as a function of temperature at 11.7 T. The analogous parameters for Gd(DOTA)$^{-}$ and the monoamide Gd(DO3AM^{pNO2Bn}) are also shown for comparison. Underlined parameters were fixed in the fit.

	Gd(DOTA)[a]	Gd(DO3AM^{pNO2Bn})[b]	Gd(DO2A2M^{nBu})	Gd(DOTA-diBPEN)[c]	Gd(DOTAM)[d]
q	1	1	1	1	1
k_{ex}^{298} (10^6 s^{-1})	4.1	1.6[e]	0.77(3)	0.72	0.05
$\Delta H^{\neq}$ (kJ.mol^{-1})	49.8	40.9	30(2)	38.0	–
$\Delta S^{\neq}$ (J.mol^{-1} K^{-1})	+48.5	+11	−33(5)	−5	–
τ_R^{298}(ps)	90	210	144(4)	375	–
E_R (kJ.mol^{-1})	16.1	17.7	19.3(6)	15	–
τ_v^{298}(ps)	11	–	2.7(2)	11	–
Δ^2(10^{20}s^{-1})	0.16	–	0.7(2)	0.16	–
A/ħ(10^6rad.s^{-1})	−3.7	−3.8	−3.8	−3.7	–
C_{os}	0.21	0.06	0.2	–	–

[a] Ref. [58].
[b] Ref. [59].
[c] Ref. [60].
[d] Ref. [19].
[e] Similar rate constant was determined for the structurally similar Gd(DO3AM^{nBu}) [15] and Gd(DO3AM$^{C5H10-CO2H}$) complexes [22].

quadrupolar coupling constant $\eta(1 + \eta^2/3)^{1/2}$ = 7.58 MHz (the value for pure water). All equations used in the fit are presented in the supporting information. A summary of all calculated parameters are given in Table 5.

The water exchange rate, 0.77 × 10^6 s^{-1}, was found to be about one fifth of that of Gd(DOTA)$^{-}$, about ½ of that measured for Gd(DO3AM^{pNO2Bn}), a DOTA-monoamide complex, and essentially identical to that measured for Gd(DOTA-diBPEN)$^{+}$, a bis-amide complex. These data are fully consistent with the previous observations that the rate of water exchange gradually decreases in proportion to the degree of carboxylate to amide substitutions [61,62]. Such decrease in k_{ex}, generally by a factor of ~3 upon the replacement of one carboxylate function by an amide, is observed in the family of both macrocyclic DOTA- and linear DTPA-type chelates (DTPA = diethylenetriamine-*N*,*N*,*N*′,*N*″,*N*″-pentaacetate). For instance, water exchange rates varies from k_{ex}^{298} = 3.3 × 10^6 s^{-1} for Gd(DTPA)$^{2-}$ to 1.3 × 10^6 s^{-1} for the monoamide and 0.43 × 10^6 s^{-1} for the bisamide derivative complexes [63].

Interestingly, the activation entropy was found to be negative. Although this would suggest an associatively activated water exchange mechanism, the attribution of the mechanism is not possible solely on the basis of the activation entropy and the activation volume would need to be measured to fully confirm that conclusion [64]. It should be noted however that the decrease in activation entropy from the large positive value in Gd(DOTA)$^{-}$ was already observed for the monoamide complex, Gd(DO3AM^{pNO2Bn}). The value of the rotational correlation time, τ_R^{298} = 144 ps, is consistent with the molecular weight of Gd(DO2A2M^{nBu})$^{+}$.

3. Summary

The present work shows that substitution of acetamide functionalities for the acetate pendant arms on DOTA significantly changes the properties of the ligand. The protonation constants of the macrocyclic amines decreases dramatically as the number of the amide pendant arms increase and, as a result, the stability of the Ln(DO2A2M^{nBu})$^{+}$ complexes are lower than those of the corresponding Ln(DOTA)$^{-}$ complexes. The rates of complex formation were also generally slower than those observed for the Ln(DOTA)$^{-}$ complexes, suggesting that the protonated LnH$_2$(DO2A2M^{nBu})$^{3+}$ intermediates formed in the initial step dissociate more slowly in these complexes. Interestingly, there were only minor differences in the rates of the acid catalyzed dissociation of the Ce(III) and Eu(III) complexes of DO2A2M^{nBu} and the corresponding Ln(DOTA)$^{-}$ complexes even though the bis(amide) chelates exhibit much lower thermodynamic stability. Keeping in mind that the Ln^{3+} complexes of DOTA-tetra(amide)s exhibit greater inertness than the Ln(DOTA)$^{-}$ complexes (especially those formed with ternary amides) one can conclude that the presence of two acetate metal binding units still allows the acid catalyzed dissociation to occur with a rate observed for the Ln(DOTA)$^{-}$ complexes. Therefore, the kinetic inertness of such complexes could be improved by further decreasing the number of protonation sites. The water exchange rate on Gd(DO2A2M^{nBu})$^{+}$, as directly assessed from the variable temperature ^{17}O transverse relaxation rates, is in accordance with a slower exchange typically observed upon replacement of carboxylate functions with amides.

4. Experimental

1,4,7,10-tetraazacyclodoecane-1,7-di(acetic acid tert-butyl ester) (DO2A-tert-butyl ester) (1). Compound (**1**) was synthesized following a literature procedure [65].

N-(Butyl)-2-bromoacetamide (2). This compound was prepared following a literature procedure [66]. K_2CO_3 (1.42 g, 10.3 mmol) dissolved in 20 mL of distilled water was added to a solution of n-butylamine (0.50 g, 6.8 mmol) in dichloromethane (15 mL). The resulting two-phase solution was cooled to 0 °C and a solution of bromoacetyl bromide (2.07 g, 10.3 mmol) in dichloromethane (10 mL) was added drop-wise over 30 min to the solution at 0 °C. The reaction mixture was stirred for 12 h at room temperature. The separated aqueous layer was washed with dichloromethane (3 × 15 mL). The combined organic layer was also washed with water (2 × 15 mL), dried over anhydrous Na_2SO_4 and evaporated by rotary evaporation to yield a colorless oil (95% yield). ^{1}H NMR (400 MHz, $CDCl_3$): δ = 0.93 (t, 3H), 1.36 (m, 2H), 1.52 (m, 2H), 3.28 (q, 2H), 3.87 (s, 2H), 6.57 (br s, 1H); ^{13}C{^{1}H} NMR (100 MHz, $CDCl_3$): 13.64, 19.92, 29.29, 31.24, 39.31, 165.26; ESI-MS: *m/z* calcd: found [M + H]$^{+}$. ESI-MS: m/z: calcd 193.01 [M]$^{+}$, found 194.01 [M + H]$^{+}$.

1,4,7,10-tetraazacyclodoecane-1,7-di(acetic acid tert-butyl ester)-4,10-di(*N*-butylacetamide) (3). 1,4,7,10-tetraazacyclodoecane-1,7-diacetic acid tert-butyl ester (**1**) (0.20 g, 0.50 mmol) was dissolved in dry acetonitrile (10 mL) and potassium carbonate (0.35 g, 2.45 mmol) was added to the solution. The suspension was heated to reflux. *N*-(Butyl)-2-bromoacetamide (**2**) (0.12 g, 1.25 mmol) dissolved in warm acetonitrile (10 mL) was added drop-wise to the refluxing solution, and the reaction was refluxed for 24 h. After allowing the suspension to cool to ambient temperature, the inorganic salts were filtered off and the solvent was removed under reduced pressure. The crude mixture was purified by column chromatography (dichloromethane/methanol, 9:1) to afford the product as a white solid.

Yield: 0.25 g, 80%. ^{1}H NMR (400 MHZ, $CDCl_3$): δ(ppm) = 0.82 (t, 6H), 1.30–1.21 (m, 4H), 1.39 (s, 18H), 1.50–1.45 (m, 4H), 2.34 (br, 8H), 2.47 (br, 8H), 2.99 (br, 4H), 3.18–3.14 (m, 4H), 3.26 (br, 4H), 7.56 (m, 2H). ^{13}C{^{1}H}NMR (100 MHz, $CDCl_3$): δ = 13.78, 20.06, 28.00, 31.73, 39.00, 50.44, 55.44, 56.52, 81.44, 171.17, 171.44. ESI-MS: *m/z*: calcd 626.14 $[M]^+$, found 627.35 $[M + H]^+$.

1,4,7,10-tetraazacyclododecane-1,7-di(acetic acid)-4,10-di(*N*-butylacetamide) (**4**). 1,4,7,10-tetraazacyclodoecane-1,7-di(acetic acid tert-butyl ester)-4,10-di(*N*-butylacetamide) (**3**) (0.20 g, 0.32 mmol) was dissolved in a mixture of dichloromethane (5 mL) and trifluoroacetic acid (5 mL) and the solution was stirred at ambient temperature for 12 h. The solvents were removed under reduced pressure, followed by repeated addition and evaporation of dichloromethane (3 × 5 mL) to remove TFA. The sticky solid product was dissolved in water, small amount of dilute HCl solution was added and the solution was and freeze dried twice to afford the product as a white solid. Yield: 0.18 g (85%); Anal. Calcd for $C_{24}H_{46}N_6O_6$ x 3HCl x $2H_2O$: C, 43.67%; H, 8.09%; N, 12.73%. Found: C, 43.74%; H, 7.78%; N, 12.40%. ^{1}H NMR (400 MHz, D_2O): δ(ppm) = 0.76 (t, 6H), 1.24–1.14 (m, 4H), 1.41–1.33 (m, 4H), 3.11 (br, 12H), 3.29 (br, 8H), 3.55 (br, 4H), 3.88 (br, 4H). ^{13}C{^{1}H} NMR (100 MHz, D_2O): δ =13.61, 20.13, 30.29, 31.10, 40.10, 48.43, 50.95, 52.88, 53.44, 56.05, 163.42, 163.78; ESI-MS: m/z: calcd 514.35 $[M]^+$, found 515.29 $[M + H]^+$.

4.1. Equilibrium studies

Stock solutions of the metal chlorides were prepared by dissolving ACS reagent grade salts in triple distilled water. The concentration of metal and ligand stock solutions were determined by using known titrimetric methods. The stability and protonation constants the ligands and complexes formed with DO2A2M^{nBu} chelator were determined by pH-potentiometric method. The stability and protonation constants determinations on the Cu^{2+} system were also supported by UV–vis spectrophotometry. pH-potentiometric titrations were performed by using samples with metal-to-ligand concentration ratios 1:1 and 2:1 (the concentration of the ligand in the samples was generally 0.002 or 0.003 M). pH-potentiometric titrations were carried out using a Thermo Orion ion analyzer EA940 pH meter using a 6.0234.100 Metrohm combined electrode in a mixing vessel thermostated at 25.0 °C. A Metrohm DOSIMATE 665 autoburette (5 mL capacity) was used for base additions and 1.0 M KCl was used to maintain the ionic strength (1.0 M NaCl in case of Cu^{2+}). All equilibrium measurements (direct titrations) were carried out in 6.00 mL samples with magnetic stirring. During the titrations, argon gas was passed over the sample to maintain the cell free of CO_2. The electrodes were calibrated according to the standard two point calibration procedure with commercially available buffers (0.01 M borax, pH = 9.180 and 0.05 M KH-phthalate, pH = 4.005). The concentrations of H^+ ions were calculated from the measured pH values using the method proposed by Irving et al. [67] This method involves the titration of diluted stock solutions of HCl (approx. 0.027 M in 1.0 M KCl/NaCl) with standardized KOH/NaOH solutions. The difference between the measured and calculated pH was then used to correct the pH values obtained in the titration experiments. The log K_w of water was also calculated from these titration data and was found to be 13.868.

The UV–vis stability constant of the Cu(DO2AM^{nBu}) complex was determined by spectrophotometry by studying the Cu^{2+} - DO2AM^{nBu} system at the absorption band of the Cu^{2+} complexes in the $[H^+]$ range of 0.0117–1.02 M and in the wavelength range of 400–875 nm ([NaCl] + [HCl] = 1.0 M). The concentration of Cu^{2+} and the ligands in these samples was 0.003 M. The H^+ concentration in the samples was adjusted with the addition of standardized 2.0109 M HCl. The samples were kept at 25 °C for a week in order to achieve the full equilibration. The absorbance values of the samples were determined at 26 different wavelength values in the range of 600–850 nm. For the equilibrium calculations of the stability and protonation constants the molar absorptivities of the $CuCl_2$ and Cu(DO2AM^{nBu}) were determined independently using 0.0015 M, 0.003 M and 0.0045 M solutions. The spectrophotometric experiments were performed with JASCO V770 UV–Vis-NIR spectrophotometer and 1 cm quartz semi-micro cuvettes at 25 °C.

Owing to the slow formation reactions of Ln(DO2AM^{nBu}) complexes, the "out-of-cell" titration method (also known as the batch method) was applied for the stability constant determinations of these chelates. Typically, a 3.0 mL mixture of Ln(III) and ligand (both at 3.0 mM concentration) were prepared and the pH was adjusted with HCl or KOH to cover the pH range of 1.7–3.5 where complexation takes place as predicted by model calculations. Typically 16 samples were prepared sealed and placed in a 25 °C incubator for 90 days to ensure that the samples reached equilibrium. UV–vis experiments performed on the samples with Ce(III) indicated that this time period was sufficient for the samples to reach equilibrium (as further measurements performed on the 120th day indicated no change in the UV spectra of the reaction mixture). The pH of the samples were then measured and the data processed. The protonation and stability constants were calculated with the program PSEQUAD. [68]

4.2. Formation kinetics

The rates of complex formation of Ln(DO2AM^{nBu}) complexes were studied at 25 °C and 1.0 M KCl ionic strength using Cary 300 Bio UV–Vis spectrophotometer. The formation reactions at low pH were sufficiently slow and were followed by conventional UV–vis spectroscopy. A typical concentration of DO2AM^{nBu} was 0.5 mM while the concentration of the metal ions was varied in between 5.0 and 55.0 mM (10 to 110 fold metal excess) when the saturation curves were recorded. The formation reactions with Ce and Eu were studied in the pH range of 4.37–5.81 while the studies involving Yb were performed in the pH range of 3.97–5.26. The reactions were followed at 322 (Ce) and 250 nm (Eu). The formation rate of Yb(DO2A2M^{nBu})$^+$ complex was studied by the "indicator method" [49]. This involved the preparation of weakly buffered solutions in which the complex formation led to pH changes of about 0.025–0.05 pH unit. The changes in pH were followed by spectrophotometry with the use of an acid – base indicator such as bromocresol green (615 nm) or bromocresol purple (590 nm). During the formation kinetic studies the non-coordinating buffers *N*-methylpiperazine (NMP, log K_2^H = 4.83) and *N,N'*-dimethylpiperazine (DMP, log K_2^H = 4.18) were applied at a concentration of 0.05 M (Ce(III) and Eu (III)) or was experimentally determined (typically it was in the range of 0.025–0.035 M for the (III)) to maintain the pH constant.

$$A_t = A_e + (A_0 - A_e)\cdot e^{(-k_{obs}\cdot t)} \quad (5)$$

Eq. (5) was used to calculate the first order rate constants (k_{obs} for formation and k_d for dissociation), where A_0, A_e and A_t are the absorbance values measured at the start of the reaction (t = 0), at equilibrium and at time t, respectively.

4.3. Kinetics of dissociation

The acid catalyzed dissociation kinetics of Ce(DO2AM^{nBu})$^+$ and Eu (DO2AM^{nBu})$^+$ complexes were measured under pseudo-first-order conditions by mixing the appropriate complexes with large excess of hydrochloric acid (0.25–2.0 M) while keeping the ionic strength constant at 2.0 M with added KCl $[(H^+ + K^+)Cl^-]$. A total of 8–10 reactions were followed by direct spectrophotometry at 25 °C until the conversion reached 80–100% in 1.0 mM complex solutions. The data were fitted to Eq. 5 with the software Scientist (Micromath) using a standard least square procedure.

4.4. Temperature-dependent ^{17}O NMR measurements

Transverse and longitudinal ^{17}O relaxation rates ($1/T_2$, $1/T_1$) and

chemical shifts were measured in aqueous solutions of GdL (0.028 mM, pH = 6.84) in the temperature range 277-340 K, on a Bruker Avance 500 (11.7 T, 67.8 MHz) spectrometer. The temperature was calculated according to previous calibration with ethylene glycol and methanol [69]. An acidified water solution ($HClO_4$, pH 3.3) was used as external reference. Longitudinal relaxation times (T_1) were obtained by the inversion-recovery method, and transverse relaxation times (T_2) were obtained by the Carr-Purcell-Meiboom-Gill (CPMG) spin-echo technique [70]. The technique of the ^{17}O NMR measurements on Gd^{3+} complexes has been described elsewhere [71]. The samples were sealed in glass spheres fitted into 10 mm NMR tubes to avoid susceptibility corrections of the chemical shifts [72]. To improve the sensitivity, ^{17}O-enriched water (10% $H_2{}^{17}O$, CortectNet) was added to the solutions to reach around 2% enrichment. The ^{17}O NMR data have been treated according to the Solomon-Bloembergen-Morgan theory of paramagnetic relaxation (see Supporting Information). The least-squares fit of the ^{17}O NMR data were performed using Visualiseur/Optimiseur running on a MATLAB 8.3.0 (R2014a) platform [73].

Abbreviations

MRI Magnetic Resonance Imaging
CAs contrast agents
DO2A2M^{nBu} 1,4,7,10-tetraazacyclododecane-1,7-di(acetic acid)-4,10-di(*N*-butylacetamide)
Ln(III) ions lanthanide(III) ions
DOTA 1,4,7,10-tetraazacyclododecane-1,4,7,10-tetraacetic acid
HP-DO3A 2,2′,2″-[10-(2-hydroxypropyl)-1,4,7,10-tetraazacyclododecane-1,4,7-triyl]triacetic acid
DO3A-butrol 10-(2,3-dihydroxy-1-hydroxymethylpropyl)-1,4,7,10-tetraazacyclododecane-1,4,7-triacetic acid
DOTAM 1,4,7,10-tetrakis(carbamoylmethyl)-1,4,7,10-tetraazacyclododecane
DTMA 1,4,7,10-tetra(methylcarbamoylmethyl)-1,4,7,10-tetraazacyclodoecane
RNA ribonucleic acid
SAP square antiprism
TSAP twisted square antiprism
paraCEST paramagnetic chemical exchange saturation transfer
DPA *N*,*N*-bis(2-pyridyl-methyl)ethylene diamine or di-(2-picolyl) amine
HSA human serum albumin
DO2A-tert-butyl ester 1,4,7,10-tetraazacyclodoecane-1,7-di(acetic acid tert-butyl ester)
TFA trifluoroacetic acid
DO3AM^{nBu} 1,4,7,10-tetraazacyclodoecane-1,4,7-tri(acetic acid)-10-(*N*-butylacetamide)
DO2A 1,4,7,10-tetraazacyclodoecane-1,7-di(acetic acid)
DOTA-(gly)$_4$ 1,4,7,10-tetraazacyclododecane-1,4,7,10-tetrakis(acetamidoacetic acid)
DTPA diethylenetriamine-*N*,*N*,*N*′,*N*″,*N*″-pentaacetate
NMP *N*-methylpiperazine
DMP *N*,*N*′-dimethylpiperazine
T_1 longitudinal relaxation time
T_2 transverse relaxation time
CPMG Carr-Purcell-Meiboom-Gill

Declaration of competing interest

The authors declare no conflict of interest.

Acknowledgements

The authors acknowledge financial support from the Hungarian National Research Development and Innovation Office (NKFIH K-120224 and 128201 projects) and the COST Action CA15209 European Network on NMR Relaxometry. The research was also supported in a part by the EU and co-financed by the European Regional Development Fund under the project GINOP-2.3.2-15-2016-00008, and by the Robert A. Welch Foundation (grant AT-586) of Houston, Texas.

Appendix A. Supplementary data

Supplementary data to this article: definition of protonation/stability constants, mechanism of formation of Ln^{3+} complexes, absorption spectra of the Cu^{2+}–DO2A2M^{nBu} system, pseudo-first-order rate constants (k_{obs}) for the formation of Yb(DO2A2MnBu)$^+$ and dependence of k_{obs} values on the buffer concentration for the formation of Ce^{3+}, Eu^{3+} and Yb^{3+} complexes of DO2A2MnBu, ^1H- and ^{13}C-NMR data of the new compounds synthesized, equations used for the fit of ^{17}O-NMR data can be found online at https://doi.org/10.1016/j.jinorgbio.2020.111042.

References

[1] E. Brucher, Z. Baranyai, G. Tircso, The Future of Biomedical Imaging: Synthesis and Chemical Properties of the DTPA and DOTA Derivative Ligands and Their Complexes, RSC Drug Discov. Ser. No 15 Biomed. Imaging Chem. Labels Probes Contrast Agents Publ. R. Soc. Chem. 44 (2012) 208–260. doi:https://doi.org/10.1002/chin.201312241.
[2] T.J. Clough, L. Jiang, K.-L. Wong, N.J. Long, Ligand design strategies to increase stability of gadolinium-based magnetic resonance imaging contrast agents, Nat. Commun. 10 (2019) 1420, https://doi.org/10.1038/s41467-019-09342-3.
[3] J. Wahsner, E.M. Gale, A. Rodríguez-Rodríguez, P. Caravan, Chemistry of MRI contrast agents: current challenges and new frontiers, Chem. Rev. 119 (2019) 957–1057, https://doi.org/10.1021/acs.chemrev.8b00363.
[4] P. Caravan, J.J. Ellison, T.J. McMurry, R.B. Lauffer, Gadolinium (III) chelates as MRI contrast agents: structure, dynamics, and applications, Chem. Rev. 99 (1999) 2293–2352, https://doi.org/10.1021/cr980440x.
[5] L. Helm, A.E. Merbach, É. Tóth (Eds.), The Chemistry of Contrast Agents in Medical Magnetic Resonance Imaging, Second edition, John Wiley & Sons Inc, Hoboken, NJ, 2013.
[6] M. Le Fur, P. Caravan, The biological fate of gadolinium-based MRI contrast agents: a call to action for bioinorganic chemists, Metallomics 11 (2019) 240–254, https://doi.org/10.1039/C8MT00302E.
[7] G.-P. Yan, L. Robinson, P. Hogg, Magnetic resonance imaging contrast agents: overview and perspectives, Radiography 13 (2007) e5–e19, https://doi.org/10.1016/j.radi.2006.07.005.
[8] S. Aime, P. Caravan, Biodistribution of gadolinium-based contrast agents, including gadolinium deposition, J. Magn. Reson. Imaging 30 (2009) 1259–1267, https://doi.org/10.1002/jmri.21969.
[9] A.D. Sherry, P. Caravan, R.E. Lenkinski, Primer on gadolinium chemistry, J. Magn. Reson. Imaging 30 (2009) 1240–1248, https://doi.org/10.1002/jmri.21966.
[10] S. Aime, S.G. Crich, M. Botta, G. Giovenzana, G. Palmisano, M. Sisti, A macromolecular Gd(III) complex as pH-responsive relaxometric probe for MRI applications, Chem. Commun. (1999) 1577–1578, https://doi.org/10.1039/a900499h.
[11] J.-A. Park, J.-J. Lee, J.-C. Jung, D.-Y. Yu, C. Oh, S. Ha, T.-J. Kim, Y. Chang, Gd-DOTA conjugate of RGD as a potential tumor-targeting MRI contrast agent, ChemBioChem 9 (2008) 2811–2813, https://doi.org/10.1002/cbic.200800529.
[12] T.L. Kalber, N. Kamaly, P.-W. So, J.A. Pugh, J. Bunch, C.W. McLeod, M.R. Jorgensen, A.D. Miller, J.D. Bell, A low molecular weight folate receptor targeted contrast agent for magnetic resonance tumor imaging, Mol. Imaging Biol. 13 (2011) 653–662, https://doi.org/10.1007/s11307-010-0400-3.
[13] L.M. De León-Rodríguez, A. Ortiz, A.L. Weiner, S. Zhang, Z. Kovacs, T. Kodadek, A.D. Sherry, Magnetic resonance imaging detects a specific peptide−protein binding event, J. Am. Chem. Soc. 124 (2002) 3514–3515, https://doi.org/10.1021/ja025511v.
[14] L. Frullano, C. Wang, R.H. Miller, Y. Wang, A myelin-specific contrast agent for magnetic resonance imaging of myelination, J. Am. Chem. Soc. 133 (2011) 1611–1613, https://doi.org/10.1021/ja1040896.
[15] F.A. Rojas-Quijano, G. Tircsó, E. Tircsóné Benyó, Z. Baranyai, H. Tran Hoang, F.K. Kálmán, P.K. Gulaka, V.D. Kodibagkar, S. Aime, Z. Kovács, A.D. Sherry, Synthesis and characterization of a hypoxia-sensitive MRI probe, Chem. Eur. J. 18 (2012) 9669–9676, https://doi.org/10.1002/chem.201200266.
[16] P. Caravan, P. Mehrkhodavandi, C. Orvig, Cationic lanthanide complexes of *N*,*N*′-bis(2-pyridylmethyl)ethylenediamine-*N*,*N*′-diacetic acid (H_2 bped), Inorg. Chem. 36 (1997) 1316–1321. doi:https://doi.org/10.1021/ic9613016.
[17] A.D. Sherry, R.D. Brown, C.F.G.C. Geraldes, S.H. Koenig, K.-T. Kuan, M. Spiller, Synthesis and characterization of the gadolinium (3+) complex of DOTA-propylamide: a model DOTA-protein conjugate, Inorg. Chem. 28 (1989) 620–622, https://doi.org/10.1021/ic00302a049.
[18] L. Tei, Z. Baranyai, L. Gaino, A. Forgács, A. Vágner, M. Botta, Thermodynamic stability, kinetic inertness and relaxometric properties of monoamide derivatives of lanthanide(III) DOTA complexes, Dalton Trans. 44 (2015) 5467–5478, https://doi.org/10.1039/C4DT03939D.
[19] S. Aime, A. Barge, J.I. Bruce, M. Botta, J.A.K. Howard, J.M. Moloney, D. Parker, A.S. de Sousa, M. Woods, NMR, relaxometric, and structural studies of the

hydration and exchange dynamics of cationic lanthanide complexes of macrocyclic tetraamide ligands, J. Am. Chem. Soc. 121 (1999) 5762–5771, https://doi.org/10.1021/ja990225d.
[20] A. Pasha, G. Tircsó, E.T. Benyó, E. Brücher, A.D. Sherry, Synthesis and characterization of DOTA-(amide)4 derivatives: equilibrium and kinetic behavior of their lanthanide (III) complexes, Eur. J. Inorg. Chem. 2007 (2007) 4340–4349, https://doi.org/10.1002/ejic.200700354.
[21] S. Amin, J.R. Morrow, C.H. Lake, M.R. Churchill, Lanthanide(III) tetraamide macrocyclic complexes as synthetic ribonucleases: structure and catalytic properties of [La(tcmc)(CF3SO3)(EtOH)](CF3SO3)2, Angew. Chem. Int. Ed. Engl. 33 (1994) 773–775, https://doi.org/10.1002/anie.199407731.
[22] Crich Geninatti, C. Cabella, A. Barge, S. Belfiore, C. Ghirelli, L. Lattuada, S. Lanzardo, A. Mortillaro, L. Tei, M. Visigalli, G. Forni, S. Aime, In vitro and in vivo magnetic resonance detection of tumor cells by targeting glutamine transporters with Gd-based probes, J. Med. Chem. 49 (2006) 4926–4936, https://doi.org/10.1021/jm0601093.
[23] Z. Baranyai, E. Brücher, T. Iványi, R. Király, I. Lázár, L. Zékány, Complexation properties of *N,N′,N″,N‴*-[1,4,7,10-tetraazacyclododecane-1,4,7,10-tetrayltetrakis (1-oxoethane-2,1-diyl)]tetrakis[glycine] (H_4 dotagl). Equilibrium, kinetic, and relaxation behavior of the lanthanide(III) complexes, Helv. Chim. Acta. 88 (2005) 604–617. doi:https://doi.org/10.1002/hlca.200590042.
[24] S. Aime, A. Barge, D. Delli Castelli, F. Fedeli, A. Mortillaro, F.U. Nielsen, E. Terreno, Paramagnetic lanthanide(III) complexes as pH-sensitive chemical exchange saturation transfer (CEST) contrast agents for MRI applications, Magn. Reson. Med. 47 (2002) 639–648.
[25] G. Angelovski, T. Chauvin, R. Pohmann, N.K. Logothetis, É. Tóth, Calcium-responsive paramagnetic CEST agents, Bioorg. Med. Chem. 19 (2011) 1097–1105, https://doi.org/10.1016/j.bmc.2010.07.023.
[26] A.C. Esqueda, J.A. López, G. Andreu-de-Riquer, J.C. Alvarado-Monzón, J. Ratnakar, A.J.M. Lubag, A.D. Sherry, L.M. De León-Rodríguez, A new gadolinium-based MRI zinc sensor, J. Am. Chem. Soc. 131 (2009) 11387–11391, https://doi.org/10.1021/ja901875v.
[27] A.J.M. Lubag, L.M. De Leon-Rodriguez, S.C. Burgess, A.D. Sherry, Noninvasive MRI of -cell function using a Zn2 + -responsive contrast agent, Proc. Natl. Acad. Sci. 108 (2011) 18400–18405, https://doi.org/10.1073/pnas.1109649108.
[28] L.M. De León-Rodríguez, A.J.M. Lubag, J.A. López, G. Andreu-de-Riquer, J.C. Alvarado-Monzón, A.D. Sherry, A second generation MRI contrast agent for imaging zinc ions in vivo, MedChemComm 3 (2012) 480, https://doi.org/10.1039/c2md00301e.
[29] M.V. Clavijo Jordan, S.-T. Lo, S. Chen, C. Preihs, S. Chirayil, S. Zhang, P. Kapur, W.-H. Li, L.M. De Leon-Rodriguez, A.J.M. Lubag, N.M. Rofsky, A.D. Sherry, Zinc-sensitive MRI contrast agent detects differential release of Zn(II) ions from the healthy vs. malignant mouse prostate, Proc. Natl. Acad. Sci. 113 (2016) E5464–E5471. https://doi.org/10.1073/pnas.1609450113.
[30] Zhang, S., Kovacs, Z., Burgess, S., Aime, S., Terreno, E., Sherry, A. D., {DOTA-bis (amide)}lanthanide complexes: NMR evidence for differences in water-molecule exchange rates for coordination isomers, Chem. Eur. J. 7 (2001) 288.
[31] L.G. Nielsen, T.J. Sørensen, Including and declaring structural fluctuations in the study of lanthanide(III) coordination chemistry in solution, Inorg. Chem. 59 (2020) 94–105, https://doi.org/10.1021/acs.inorgchem.9b01571.
[32] G. Anderegg, F. Arnaud-Neu, R. Delgado, J. Felcman, K. Popov, Critical evaluation of stability constants of metal complexes of complexones for biomedical and environmental applications* (IUPAC technical report), Pure Appl. Chem. 77 (2005) 1445–1495, https://doi.org/10.1351/pac200577081445.
[33] J. Huskens, D.A. Torres, Z. Kovacs, J.P. André, C.F.G.C. Geraldes, A.D. Sherry, Alkaline earth metal and lanthanide(III) complexes of ligands based upon 1,4,7,10-tetraazacyclododecane-1,7-bis(acetic acid), Inorg. Chem. 36 (1997) 1495–1503, https://doi.org/10.1021/ic961131x.
[34] J.M. Weeks, M.R. Taylor, K.P. Wainwright, Formation constants for complexes of 1,4,7,10-tetraazacyclododecane-1,7-diacetic acid and the crystal structure of its nickel (II) complex, J. Chem. Soc. Dalton Trans. (1997) 317–322, https://doi.org/10.1039/a605208h.
[35] C.A. Chang, Y.-H. Chen, H.-Y. Chen, F.-K. Shieh, Capillary electrophoresis, potentiometric and laser excited luminescence studies of lanthanide(III) complexes of 1,7-dicarboxymethyl-1,4,7,10-tetraazacyclododecane (DO2A)†, J. Chem. Soc. Dalton Trans. (1998) 3243–3248, https://doi.org/10.1039/a803565b.
[36] H. Maumela, R.D. Hancock, L. Carlton, J.H. Reibenspies, K.P. Wainwright, The amide oxygen as a donor group. metal ion complexing properties of tetra-N-acetamide substituted cyclen: a crystallographic, NMR, molecular mechanics, and thermodynamic study, J. Am. Chem. Soc. 117 (1995) 6698–6707. doi:https://doi.org/10.1021/ja00130a008.
[37] J.F. Desreux, E. Merciny, M.F. Loncin, Nuclear magnetic resonance and potentiometric studies of the protonation scheme of two tetraaza tetraacetic macrocycles, Inorg. Chem. 20 (1981) 987–991, https://doi.org/10.1021/ic50218a008.
[38] J.F. Desreux, Nuclear magnetic resonance spectroscopy of lanthanide complexes with a tetraacetic tetraaza macrocycle. Unusual conformation properties, Inorg. Chem. 19 (1980) 1319–1324. doi:https://doi.org/10.1021/ic50207a042.
[39] A. Riesen, M. Zehnder, T.A. Kaden, Metal complexes of macrocyclic ligands. Part XXIII. Synthesis, properties, and structures of mononuclear complexes with 12- and 14-membered tetraazamacrocycle-N,N′,N″,N‴-tetraacetic Acids, Helv. Chim. Acta. 69 (1986) 2067–2073. doi:https://doi.org/10.1002/hlca.19860690830.
[40] A. Riesen, M. Zehnder, T.A. Kaden, Metal complexes of macrocyclic ligands. Part XXIV. Binuclear complexes with tetraazamacrocycle-NN′,N″,N‴-tetraacetic acids, Helv. Chim. Acta. 69 (1986) 2074–2080. doi:https://doi.org/10.1002/hlca.19860690831.
[41] C. Paul-Roth, K.N. Raymond, Amide functional group contribution to the stability of gadolinium(III) complexes: DTPA derivatives, Inorg. Chem. 34 (1995) 1408–1412, https://doi.org/10.1021/ic00110a019.
[42] W.P. Cacheris, S.K. Nickle, A.D. Sherry, Thermodynamic study of lanthanide complexes of 1,4,7-triazacyclononane-N,N′,N″-triacetic acid and 1,4,7,10-tetraazacyclododecane-N,N′,N″,N‴-tetraacetic acid, Inorg. Chem. 26 (1987) 958–960. doi:https://doi.org/10.1021/ic00253a038.
[43] A. Pasha, M. Lin, G. Tircsó, C.L. Rostollan, M. Woods, G.E. Kiefer, A.D. Sherry, X. Sun, Synthesis and evaluation of lanthanide ion DOTA–tetraamide complexes bearing peripheral hydroxyl groups, JBIC J. Biol. Inorg. Chem. 14 (2009) 421–438, https://doi.org/10.1007/s00775-008-0459-3.
[44] E. Toth, E. Brucher, I. Lazar, I. Toth, Kinetics of formation and dissociation of lanthanide(III)-DOTA complexes, Inorg. Chem. 33 (1994) 4070–4076, https://doi.org/10.1021/ic00096a036.
[45] S.L. Wu, W.D. Horrocks, Kinetics of complex formation by macrocyclic polyaza polycarboxylate ligands: detection and characterization of an intermediate in the Eu3 + -dota system by laser-excited luminescence, Inorg. Chem. 34 (1995) 3724–3732, https://doi.org/10.1021/ic00118a020.
[46] L. Burai, I. Fábián, R. Király, E. Szilágyi, E. Brücher, Equilibrium and kinetic studies on the formation of the lanthanide(III) complexes, [Ce(dota)] − and [Yb(dota)] − (H4dota = 1,4,7,10-tetraazacyclododecane-1,4,7,10-tetraacetic acid), J. Chem. Soc. Dalton Trans. (1998) 243–248, https://doi.org/10.1039/a705158a.
[47] Z. Baranyai, I. Bányai, E. Brücher, R. Király, E. Terreno, Kinetics of the formation of [Ln(DOTAM)]3 + complexes, Eur. J. Inorg. Chem. 2007 (2007) 3639–3645, https://doi.org/10.1002/ejic.200700178.
[48] R.G. Wilkins, R.G. Wilkins, Kinetics and Mechanism of Reactions of Transition Metal Complexes, 2nd thoroughly rev. ed, VCH, Weinheim; New York, 1991.
[49] S.P. Kasprzyk, R.G. Wilkins, Kinetics of interaction of metal ions with two tetraazatetraacetate macrocycles, Inorg. Chem. 21 (1982) 3349–3352, https://doi.org/10.1021/ic00139a018.
[50] E. Szilágyi, É. Tóth, Z. Kovács, J. Platzek, B. Radüchel, E. Brücher, Equilibria and formation kinetics of some cyclen derivative complexes of lanthanides, Inorganica Chim. Acta. 298 (2000) 226–234, https://doi.org/10.1016/S0020-1693(99)00467-3.
[51] X. Wang, T. Jin, V. Comblin, A. Lopez-Mut, E. Merciny, J.F. Desreux, A kinetic investigation of the lanthanide DOTA chelates. Stability and rates of formation and of dissociation of a macrocyclic gadolinium (III) polyaza polycarboxylic MRI contrast agent, Inorg. Chem. 31 (1992) 1095–1099. doi:https://doi.org/10.1021/ic00032a034.
[52] K. Kumar, M.F. Tweedle, Ligand basicity and rigidity control formation of macrocyclic polyamino carboxylate complexes of gadolinium(III), Inorg. Chem. 32 (1993) 4193–4199, https://doi.org/10.1021/ic00072a008.
[53] A. Takács, R. Napolitano, M. Purgel, A.C. Bényei, L. Zékány, E. Brücher, I. Tóth, Z. Baranyai, S. Aime, Solution structures, stabilities, kinetics, and dynamics of DO3A and DO3A–sulphonamide complexes, Inorg. Chem. 53 (2014) 2858–2872, https://doi.org/10.1021/ic4025958.
[54] L. Helm, A.E. Merbach, Water exchange on metal ions: experiments and simulations, Coord. Chem. Rev. 187 (1999) 151–181, https://doi.org/10.1016/S0010-8545(99)90232-1.
[55] Z. Baranyai, Z. Pálinkás, F. Uggeri, A. Maiocchi, S. Aime, E. Brücher, Dissociation kinetics of open-chain and macrocyclic gadolinium(III)-aminopolycarboxylate complexes related to magnetic resonance imaging: catalytic effect of endogenous ligands, Chem. Eur. J. 18 (2012) 16426–16435, https://doi.org/10.1002/chem.201202930.
[56] M. Port, J.-M. Idée, C. Medina, C. Robic, M. Sabatou, C. Corot, Efficiency, thermodynamic and kinetic stability of marketed gadolinium chelates and their possible clinical consequences: a critical review, BioMetals 21 (2008) 469–490, https://doi.org/10.1007/s10534-008-9135-x.
[57] C.A. Chang, Y.-L. Liu, Dissociation kinetics of cerium(lll) complexes of macrocyclic polyaza polycarboxylate ligands TETA and DOTA, J. Chin. Chem. Soc. 47 (2000) 1001–1006, https://doi.org/10.1002/jccs.200000139.
[58] D.H. Powell, O.M.N. Dhubhghaill, D. Pubanz, L. Helm, Y.S. Lebedev, W. Schlaepfer, A.E. Merbach, Structural and dynamic parameters obtained from ^{17}O NMR, EPR, and NMRD studies of monomeric and dimeric Gd^{3+} complexes of interest in magnetic resonance imaging: an integrated and theoretically self-consistent approach[1], J. Am. Chem. Soc. 118 (1996) 9333–9346, https://doi.org/10.1021/ja961743g.
[59] É. Tóth, D. Pubanz, S. Vauthey, L. Helm, A.E. Merbach, The role of water exchange in attaining maximum relaxivities for dendrimeric MRI contrast agents, Chem. Eur. J. 2 (1996) 1607–1615, https://doi.org/10.1002/chem.19960021220.
[60] J. Yu, A.F. Martins, C. Preihs, V. Clavijo Jordan, S. Chirayil, P. Zhao, Y. Wu, K. Nasr, G.E. Kiefer, A.D. Sherry, Amplifying the sensitivity of zinc(II) responsive MRI contrast agents by altering water exchange rates, J. Am. Chem. Soc. 137 (2015) 14173–14179, https://doi.org/10.1021/jacs.5b09158.
[61] E. Brücher, G. Tircsó, Z. Baranyai, Z. Kovács, A.D. Sherry, Stability and toxicity of contrast agents, in: A. Merbach, L. Helm, É. Tóth (Eds.), Chem, Contrast Agents Med. Magn. Reson. Imaging, John Wiley & Sons, Ltd, Chichester, UK, 2013, pp. 157–208, , https://doi.org/10.1002/9781118503652.ch4.
[62] P. Caravan, D. Esteban-Gómez, A. Rodríguez-Rodríguez, C. Platas-Iglesias, Water exchange in lanthanide complexes for MRI applications. Lessons learned over the last 25 years, Dalton Trans. 48 (2019) 11161–11180. doi:https://doi.org/10.1039/C9DT01948K.
[63] É. Tóth, L. Burai, E. Brücher, A.E. Merbach, Tuning water-exchange rates on (carboxymethyl)iminobis(ethylenenitrilo)tetraacetate (dtpa)-type gadolinium(III) complexes, J. Chem. Soc. Dalton Trans. (1997) 1587–1594, https://doi.org/10.1039/a608505i.
[64] L. Helm, A.E. Merbach, Inorganic and bioinorganic solvent exchange mechanisms,

Chem. Rev. 105 (2005) 1923–1960, https://doi.org/10.1021/cr030726o.
[65] Kovacs, Z., Sherry, A. D., pH-Controlled Selective Protection of Polyaza Macrocycles, 07 (1997) 759–763.
[66] D.S.S.M. Uppu, M. Bhowmik, S. Samaddar, J. Haldar, Cyclization and unsaturation rather than isomerisation of side chains govern the selective antibacterial activity of cationic-amphiphilic polymers, Chem. Commun. 52 (2016) 4644–4647, https://doi.org/10.1039/C5CC09930G.
[67] H.M. Irving, M.G. Miles, L.D. Pettit, A study of some problems in determining the stoicheiometric proton dissociation constants of complexes by potentiometric titrations using a glass electrode, Anal. Chim. Acta 38 (1967) 475–488, https://doi.org/10.1016/S0003-2670(01)80616-4.
[68] L. Zékány, I. Nagypál, In "Computational Method for Determination of Formation Constants" Ed, Legett D J, Plenum, New York, 1985, p. 291.
[69] D.S. Raiford, C.L. Fisk, E.D. Becker, Calibration of methanol and ethylene glycol nuclear magnetic resonance thermometers, Anal. Chem. 51 (1979) 2050–2051, https://doi.org/10.1021/ac50048a040.
[70] S. Meiboom, D. Gill, Modified spin-echo method for measuring nuclear relaxation times, Rev. Sci. Instrum. 29 (1958) 688–691, https://doi.org/10.1063/1.1716296.
[71] K. Micskei, L. Helm, E. Brucher, A.E. Merbach, Oxygen-17 NMR study of water exchange on gadolinium polyaminopolyacetates [Gd(DTPA)(H2O)]2- and [Gd(DOTA)(H2O)]-related to NMR imaging, Inorg. Chem. 32 (1993) 3844–3850, https://doi.org/10.1021/ic00070a013.
[72] A.D. Hugi, L. Helm, A.E. Merbach, Water exchange on hexaaquavanadium(III): a variable-temperature and variable-pressure 17O-NMR study at 1.4 and 4.7 Tesla, Helv. Chim. Acta. 68 (1985) 508–521. doi:https://doi.org/10.1002/hlca.19850680224.
[73] Yerly, F. VISUALISEUR 2.3.5 and OPTIMISEUR 2.3.5; Lausanne, Switzerland, 1999.